Far-Infrared Spectra and Ring-Puckering Potential Energy Function of 4*H*-Pyran. Conformations and Bonding of 1,4-Cyclohexadiene and Its Oxygen Analogues

J. Choo,[†] J. Laane,[*,†] R. Majors,[‡] and J. R. Villarreal[‡]

Contribution from the Departments of Chemistry, Texas A&M University, College Station, Texas 77843, and University of Texas at Pan American, Edinburg, Texas 78539

Received March 5, 1993

Abstract: The far-infrared, mid-infrared, and Raman spectra of 4*H*-pyran have been recorded and analyzed. The far-infrared gas-phase spectrum of this molecule shows a series of 12 bands between 115 and 128 cm^{-1} arising from the ring-puckering vibration. The kinetic energy (reciprocal reduced mass) expansion was calculated for this mode and utilized in the determination of the potential energy function, which was found to be $V(cm^{-1}) = (1.21 \times 10^5)x^4 + (2.24 \times 10^4)x^2$, where x is the ring-puckering coordinate in angstroms. This shows the ring to be planar. The corresponding potential energy functions for the analogous 1,4-cyclohexadiene and 1,4-dioxin are respectively nearly harmonic and nearly quartic. Molecular mechanics (MM3) calculations satisfactorily reproduce the 1,4-cyclohexadiene potential function but underestimate the torsional forces of the C═C–O–C system in the oxygen analogues. In fact, 1,4-dioxin is incorrectly predicted to have a boat configuration. It is shown that weak π interactions between the C═C bonds and the nonbonded oxygen orbitals account for the increases in the torsional forces and the resulting potential functions.

Introduction

In recent years there have been a large number of studies of the large-amplitude ring-puckering vibrations of pseudo-four-membered rings.[1–3] The far-infrared and Raman gas-phase spectra of these large-amplitude motions have been used to determine their one-dimensional potential energy functions from which the ring conformations are readily determined. Cyclopentene was the first "pseudo-four-membered ring" to be studied.[4] It was given that designation since its ring-puckering motion resembles that of a four-membered ring in that the two olefinic carbon atoms are locked together and vibrate as a single unit during the puckering motion. Six-membered rings with two nonconjugate double bonds can also be considered as pseudo-four-membered rings because the two pairs of olefinic carbon atoms are each locked into single units. Figure 1 shows the ring-puckering coordinates for cyclobutane, cyclopentene, and 1,4-cyclohexadiene. Laane and Lord[4] observed a series of seven closely spaced bands arising from the B_{2u} ring-puckering mode of 1,4-cyclohexadiene (I) near 108 cm^{-1} in the gas-phase far-infrared spectrum. They reported that this vibration is nearly harmonic and that the conformation of the ring is planar. The gas-phase Raman overtone spectrum of this molecule confirmed this conclusion.[5] (This work corrected the erroneous conclusions from an electron diffraction study that molecule I had a boat structure.[6]) The original electron diffraction work[7] on 1,4-cyclohexadiene had, however, correctly predicted the planar conformation.

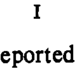
I

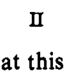
II

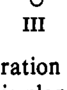
III

Lord and Rounds[8] found a series of ten strong infrared Q branches arising from the B_{2u} ring-puckering mode of 1,4-dioxin (III) in the 60–130-cm^{-1} region. They also determined the potential energy function, which was primarily quartic in character, and found III to be planar also. Strube and Laane[9] developed vector models for the ring-puckering vibrations of symmetrically substituted six-membered rings, such as I and III, and calculated the kinetic energy (reciprocal reduced mass) expansions. These functions were then used to calculate the dimensioned potential energy functions.

In order to further investigate the ring-puckering vibrations of 1,4-cyclohexadiene-like rings containing oxygen, we have analyzed the far-infrared, mid-infrared, and Raman spectra of 4*H*-pyran (II) and determined the one-dimensional potential energy function. The appropriate kinetic energy expansion was calculated and utilized for this determination. The results allow the potential energy parameters of 4*H*-pyran (II) to be compared with those of 1,4-cyclohexadiene (I) and 1,4-dioxin (III). In order to better understand the origin of each of these potential energy functions, we have also carried out molecular mechanics calculations (MM3) on all three molecules.

Experimental Section

Far-infrared spectra were recorded on a Bomem DA3.002 fourier-transform infrared interferometer equipped with a liquid helium cooled germanium bolometer as a detector. The gas-phase samples were run at 8 Torr of pressure in a Wilks multipath cell with polyethylene windows and a path length of 20.75 m. Spectra were recorded at a resolution of 0.25 cm^{-1}. Gas-phase mid-infrared spectra were recorded on a Digilab FTS-60 interferometer with use of a 10-cm gas cell with KBr windows. Liquid-phase Raman spectra were recorded on a ISA JY U-1000 monochromator equipped with a Coherent Radiation Innova 20 argon ion laser source. 4*H*-Pyran was prepared from glutardialdehyde according to the method reported by Brandsma and Arens.[10]

Results and Discussion

Vibrational Spectra. 4*H*-Pyran has three different out-of-plane ring vibrations: ν_{30}, the B_2 ring-puckering vibration; ν_{29}, the B_2

[†] Texas A&M University.

[‡] University of Texas at Pan American.

(1) Laane, J. *Pure Appl. Chem.* **1987,** *59,* 1307–1325.

(2) Carreira, L. A.; Lord, R. C.; Malloy, T. B. *Topics in Current Chemistry*; Dewar, M. J. S., et al., Eds.; Springer-Verlag: Heidelberg, 1979; Vol. 82.

(3) Legon, A. C. *Chem. Rev.* **1980,** *80,* 231–262.

(4) Laane, J.; Lord, R. C. *J. Mol. Spectrosc.* **1971,** *39,* 340–344.

(5) Carreira, L. A.; Carter, R. O.; Durig, J. R. *J. Chem. Phys.* **1973,** *59,* 812–816.

(6) Oberhammer, H.; Bauer, S. H. *J. Am. Chem. Soc.* **1969,** *91,* 10–16.

(7) Beach, J. Y. *J. Chem. Phys.* **1941,** *9,* 54–55.

(8) Lord, R. C.; Rounds, T. C. *J. Chem. Phys.* **1973,** *58,* 4344–4349.

(9) Strube, M. M.; Laane, J. *J. Mol. Spectrosc.* **1988,** *129,* 126–139.

(10) Brandsma, L.; Arens, J. F. *Recl. Trav. Chim.* **1961,** *81,* 33–34.

0002-7863/93/1515-8396$04.00/0

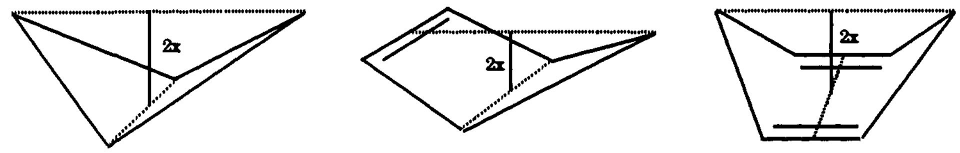

Figure 1. Ring-puckering coordinates of a four-membered ring and two pseudo-four-membered rings.

Table I. Selected Infrared and Raman Frequencies (cm^{-1}) of 4*H*-Pyran

symmetry species	vibration	assignment[a]	infrared (gas)	Raman[b] (liquid)
A_1	ν_1	=CH sym stretch (i.p.)		3078 P
	ν_3	CH_2 sym stretch	2852	2839 P
	ν_4	C=C stretch (i.p.)	1694	1690 P
	ν_5	CH_2 deformation	1455	1458
	ν_6	=CH in-plane wag (i.p.)		1213 P
	ν_8	ring stretching	1008	1011 P
	ν_9	ring stretching	880	881 P
A_2	ν_{15}	ring twisting (o.p.)		~450
B_1	ν_{17}	=CH antisym stretch (o.p.)	3076	
	ν_{18}	C=C stretch (o.p.)	1634	
	ν_{19}	ring stretching	1262	1256
	ν_{23}	ring stretching	1073	1070
	ν_{24}	ring deformation		638
B_2	ν_{25}	CH_2 antisym stretch	2929	2920
	ν_{28}	CH_2 rock	729	
	ν_{29}	ring twisting (i.p.)	481	480
	ν_{30}	ring puckering	118	

[a] i.p. = in-phase; o.p. = out-of-phase. [c] P = polarized.

in-phase ring-twisting vibration; and ν_{15}, the A_2 out-of-phase ring-twisting vibration. The ring-puckering vibration can be analyzed one dimensionally since $\nu_{15}(A_2)$ is of different symmetry and $\nu_{29}(B_2)$ is at a considerably higher frequency. As shown in Table I, ν_{30}, ν_{29}, and ν_{15} occur at 118, 481, and ~450 cm^{-1}, respectively.

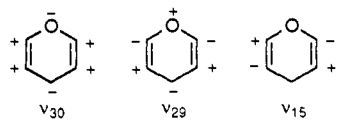

Table I also lists the fundamental infrared gas-phase and Raman liquid frequencies for some of the more intense bands of 4*H*-pyran. This molecule has C_{2v} symmetry, and the distribution of the vibrations is $11A_1 + 4A_2 + 9B_1 + 6B_2$. The mid-infrared and Raman spectra are totally consistent with C_{2v} symmetry and a planar ring conformation. More details on the spectra can be found elsewhere.[11]

The far-infrared ring-puckering spectrum of 4*H*-pyran (**II**) is shown in Figure 2. The spectrum consists of a regular series of 12 sharp Q branches, and these components were assigned as the single quantum jump transitions of the ring-puckering vibration with frequencies ranging from 115.4 (0 → 1) to 127.5 cm^{-1} (11 → 12).

Calculation of Reduced Mass. For large-amplitude motions such as the ring-puckering vibration, the reduced mass (μ) depends on the vibrational coordinate x, which is defined in Figure 1. Therefore, it is necessary to calculate the kinetic energy (reciprocal reduced mass) as a function of the conformational coordinate (the ring-puckering). Vector models for calculating the kinetic energy functions of asymmetric six-membered-ring molecules[12] have been previously developed utilizing sixth-order polynomial expansions, and these were used here. The structural parameters for the kinetic energy expansions were calculated with the MM3 molecular mechanics programs of Allinger and Burket,[13] and

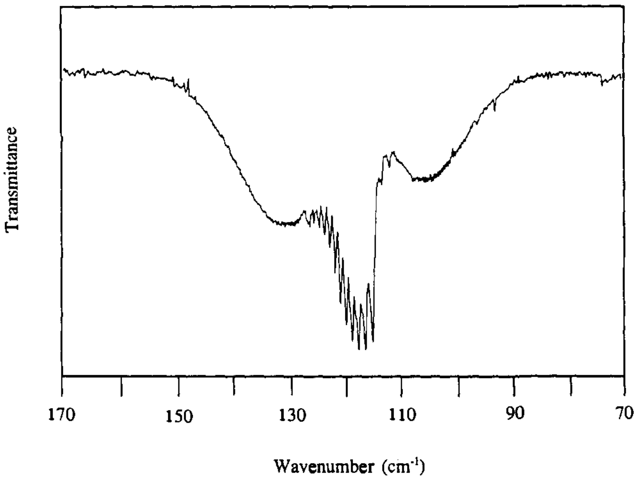

Figure 2. Far-infrared spectrum of ring-puckering vibration of 4*H*-pyran: vapor pressure, 8 Torr; path length, 20.75 m; resolution, 0.25 cm^{-1}.

Table II. Calculated Structural Parameters[a] for 4*H*-Pyran

atoms	length, Å	atoms	angle, deg
C(1)=C(2)	1.337	C(2)=C(1)—O(6)	123.5
C(2)—C(3)	1.501	C(1)=C(2)—C(3)	121.5
C(1)—O(6)	1.362	C(2)—C(3)—C(4)	111.2
C(1)—H(7)	1.103	C(1)—O(6)—C(5)	118.7
C(2)—H(8)	1.103	H(9)—C(3)—H(10)	107.6
C(3)—H(9)			

[a] From MM3 calculation.

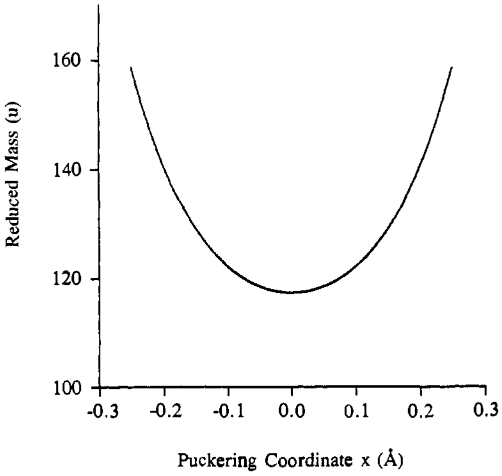

Figure 3. Plot of the variation of reduced mass for the ring-puckering vibration as a function of puckering coordinate.

these are listed in Table II. The kinetic energy terms $g_{44}(x)$ in reciprocal atomic mass units (u^{-1}) for the ring-puckering were calculated for 21 values of x in the range $-0.30 \le x \le 0.30$ Å. The calculated kinetic energy function was found to be

$$g_{44}(x) = 0.00852 - 0.03296x^2 - 0.08077x^4 + 0.66705x^6 \quad (1)$$

Figure 3 presents the variation of reduced mass with respect to the puckering coordinate of 4*H*-pyran (**II**).

Calculation of the Potential Energy Function. The Hamiltonian representing the one-dimensional ring-puckering vibration[1-3]

---

(11) Choo, J. Ph.D. Dissertation, Texas A&M University, 1993.

(12) Tecklenburg, M. M.; Laane, J. *J. Mol. Spectrosc.* **1989**, *137*, 65–81.

(13) Burkert, U.; Allinger, N. L. *Molecular Mechanics*; American Chemical Society Monograph; American Chemical Society: Washington, 1982.

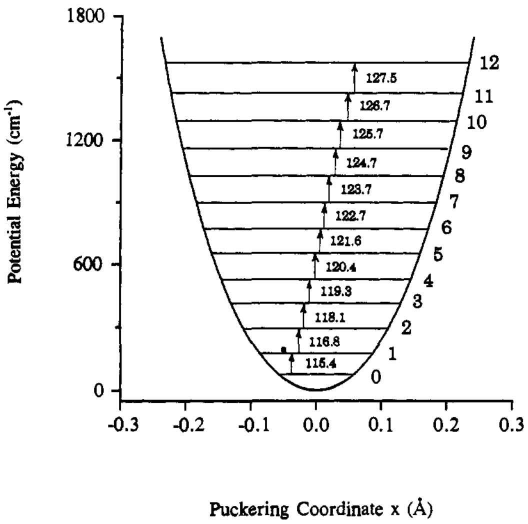

Figure 4. Plot of the ring-puckering potential energy function, the observed transitions, and the vibrational quantum states for 4*H*-pyran.

Table III. Observed and Calculated Frequencies (cm^{-1}) for Ring-Puckering Vibration of 4*H*-Pyran

transition	frequency obsd	frequency calcd[a]	Δ
$0 \rightarrow 1$	115.4	115.0	0.4
$1 \rightarrow 2$	116.8	116.6	0.2
$2 \rightarrow 3$	118.1	118.1	0.0
$3 \rightarrow 4$	119.3	119.4	-0.1
$4 \rightarrow 5$	120.4	120.7	-0.3
$5 \rightarrow 6$	121.6	121.8	-0.2
$6 \rightarrow 7$	122.7	122.9	-0.2
$7 \rightarrow 8$	123.7	123.9	-0.2
$8 \rightarrow 9$	124.7	124.8	-0.1
$9 \rightarrow 10$	125.7	125.7	0.0
$10 \rightarrow 11$	126.7	126.5	0.2
$11 \rightarrow 12$	127.5	127.2	0.3

[a] Using $V(\text{cm}^{-1}) = (1.15 \times 10^5)x^4 + (2.15 \times 10^4)x^2$ for x in angstroms.

defined by x can be expressed as

$$H(x) = (-\hbar^2/2)\, \partial/\partial x\, g_{44}(x)\, \partial/\partial x + V \qquad (2)$$

where

$$V = ax^4 + bx^2 \qquad (3)$$

and where a and b are potential energy parameters. When $b \geq 0$, the ring is planar; when $b < 0$, the ring is puckered with a barrier to planarity given by $b^2/4a$. Several computer programs available in our laboratory can be used to calculate (utilizing matrix diagonalization methods) the ring-puckering energy levels for different values of the potential energy constants. These parameters, a and b, were adjusted by least-squares refinement to fit the observed transition frequencies. The potential energy function determined for 4*H*-pyran is

$$V(\text{cm}^{-1}) = (1.21 \times 10^5)x^4 + (2.24 \times 10^4)x^2 \qquad (4)$$

where x is given in angstroms. Figure 4 shows the ring-puckering potential energy function, the observed transitions, and the ring-puckering quantum states for the molecule. The observed and calculated frequencies are compared in Table III and they show excellent agreement.

Table IV compares the potential energy constants of 4*H*-pyran (II) with those of 1,4-cyclohexadiene (I) and 1,4-dioxin (III). Figure 5 (upper left) compares the potential energy functions of the molecules. Each of these potential functions has an energy minimum at the planar conformation. As shown in Table IV, the potential energy parameters for II are intermediate between those for I and III, and the quartic character decreases in the order III > II > I. This trend reflects a mixture of contributions from ring angle strain and torsional forces for each molecule. It can be seen that the potential function of 4*H*-pyran (II) is much more similar to that of I, which has a steep potential function at small x values, than to that of III.

Table IV. Ring-Puckering Potential Energy Parameters[a] for 1,4-Cyclohexadiene (I), 4*H*-Pyran (II), and 1,4-Dioxin (III)

molecule	μ (u)	a (10^5 cm^{-1}/Å^4)	b (10^4 cm^{-1}/Å^2)	ref
$CH{=}CHCH_2CH{=}CHCH_2$ (I)	135.4	-0.37	2.37	4,9
$CH{=}CHCH_2CH{=}CHO$ (II)	117.5	1.21	2.24	this work
$CH{=}CHOCH{=}CHO$ (III)	99.7	2.86	0.34	8,9

[a] $\mu = g_{44}(0)^{-1}$ in eq 2; a and b are given in eq 3.

Molecular Mechanics Calculations and Characterization of Bonding. In order to better comprehend the origin of the planar conformations of these molecules and the nature of their potential energy functions, we have carried out molecular mechanics calculations (MM3).[13] For each molecule a series of computations was carried out to calculate the steric energies (after energy minimizations) as a function of the ring-puckering coordinates. The results based on the empirically determined force constants within the MM3 program could then be directly compared to the experimental potential energy functions.

Figure 5 (lower left) shows that the experimental and calculated functions for 1,4-cyclohexadiene (I) are in good agreement. As the molecule puckers, the angle strain at the aliphatic carbon atoms decreases as the =C–C–C= angles are reduced toward tetrahedral values. However, this decrease in angle strain is more than off-set by the torsional forces about the C–C single bonds. Thus, the lowest energy form is the planar conformation.

Figure 5 also compares the experimental and MM3 potential functions for molecules II (upper center) and III (upper right). 4*H*-Pyran (II) is correctly predicted to be planar, but 1,4-dioxin (III) is predicted to have a boat conformation. In both cases the MM3 parameters clearly underestimate the magnitude of the torsional forces which tend to keep the rings planar. As discussed below, we are convinced that the oxygen-containing molecules both have larger C=C–O–C torsional constants, due to π interactions, than in the MM3 parametrization. Moreover, these π effects should increase the "desired" C–O–C angles. To test this hypothesis, we selected the preferred C–O–C angle to be 116° (as compared to 112.4° given in the MM3 program for the =C–C–C= angle) and adjusted the V_2 2-fold torsional potential energy term until a reasonable agreement could be obtained between the experimental and calculated potential energy functions for 1,4-dioxin (III). Figure 5 (bottom right) shows that when V_2 is selected to be 0.4 kcal/mol, the experimental and calculated curves are very similar for III. When we use the same preferred angle and V_2 term in the calculation for 4*H*-pyran (II), we also get considerable improvement in the agreement between the experimental and calculated functions for this molecule as shown in Figure 5 (bottom center). For II the agreement is poorer, but a small refinement in the preferred angle and V_2 terms can produce a nearly perfect fit. In fact, the reduced symmetry of II is expected to produce somewhat different bonding interactions.

The origin of the increased torsional forces about C=C–O–C and the increase in the preferred C–O–C angle arise from interactions between the carbon–carbon π systems and the oxygen nonbonded p orbitals. We have carried out a modified Hückel calculation to better understand this. As is usual, we took each C=C interaction to have a magnitude β. In addition we set the weaker =C–O interaction to be β_w. When applied to 1,4-dioxin (III), this approach leads to the following energy states according

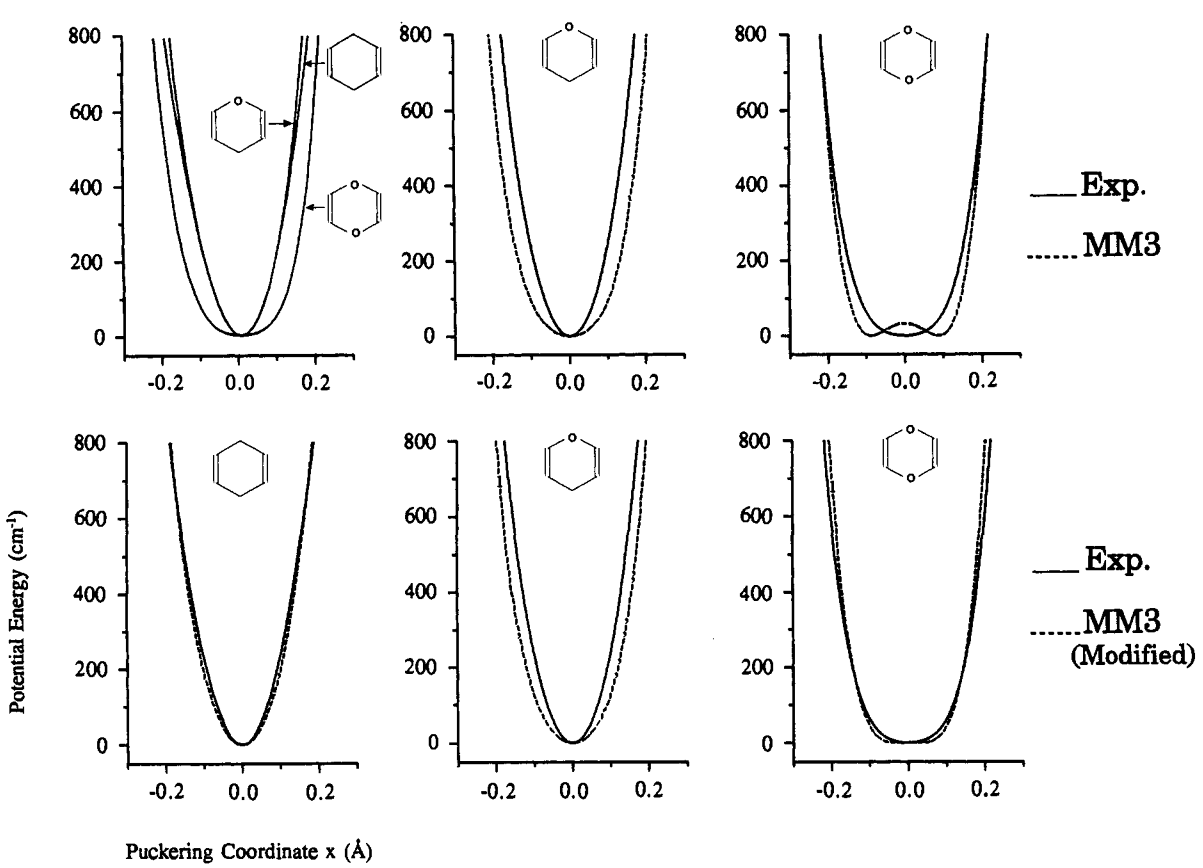

Figure 5. Comparison of the experimental ring-puckering potential energy functions of 1,4-cyclohexadiene (I), 4*H*-pyran (II), and 1,4-dioxin (III) [upper left]; experimental and calculated (from MM3) functions of II [upper center]; experimental and MM3 functions of III [upper right]; experimental and MM3 functions of I [lower left]; experimental and calculated (from modified MM3 parameters) functions of II [lower center]; experimental and modified MM3 functions of III [bottom right].

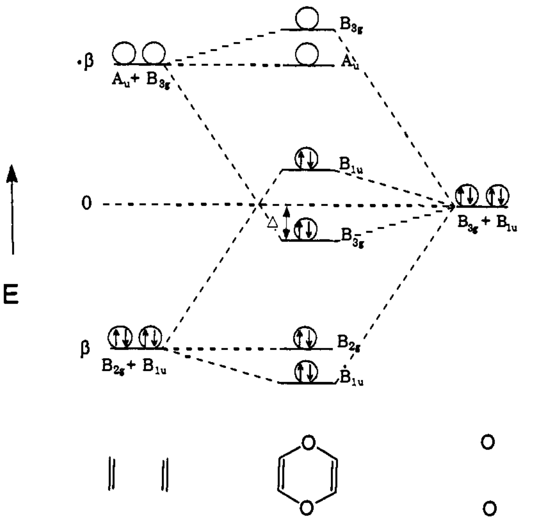

Figure 6. Molecular orbital energy levels for 1,4-dioxin (III) according to the modified Hückel calculation; Δ is a measure of the weak π interaction.

to symmetry species for the D_{2h} molecule lying the the xy plane:

$$B_{2g}: \beta \qquad A_u: -\beta$$

$$B_{3g}: -\beta/2 + (\beta^2 \pm 8\beta_w^2)^{1/2}/2 \qquad B_{1u}: \beta/2 \pm (\beta^2 + 8\beta_w^2)^{1/2}/2$$

As shown in Figure 6, the effect of the β_w interactions involving the oxygen atoms is to stabilize the filled B_{1u} π-bonding orbital while destabilizing the filled B_{1u} oxygen nonbonded p orbital by the same amount. This results in no net stabilizaiton. However, the interaction between the B_{3g} π* empty antibonding orbital and the filled B_{3g} nonbonded orbital stabilizes the latter by an amount Δ with no simultaneous destabilization. The magnitude of Δ is equal to the B_{3g} energy (with the + sign) given above. For illustrative purposes, if $\beta_w = \beta/4$ (or about 15 kcal/mol) then $\Delta = 0.112\beta$. What is important is that any interaction whatsoever will favor the planar conformation and thereby increase the C=C–O–C torsional force constant V_2 and increase the magnitude of the C–O–C angle. These were the assumptions utilized above when we fit the calculated potential function to the experimental one. Figure 7 shows graphically the B_{3g} π* to nonbonded oxygen p orbital interaction.

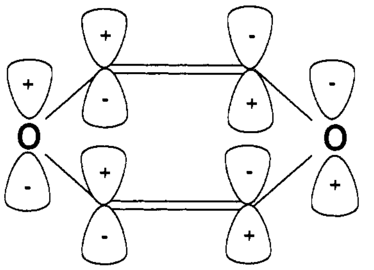

Figure 7. Bonding interaction stabilizing the planar conformation of 1,4-dioxin (III).

A similar modified Hückel calculation can be carried out for 4*H*-pyran. Here only one oxygen nonbonded p orbital is available for interaction with the two C=C double bonds. The calculated orbital energies for the C_{2v} molecule in the xz plane are

$$A_2: \pm\beta$$

$$B_2: 0, \pm(\beta^2 + 2\beta_w^2)^{1/2}$$

Figure 8 shows the orbital energy diagram. It can be seen that

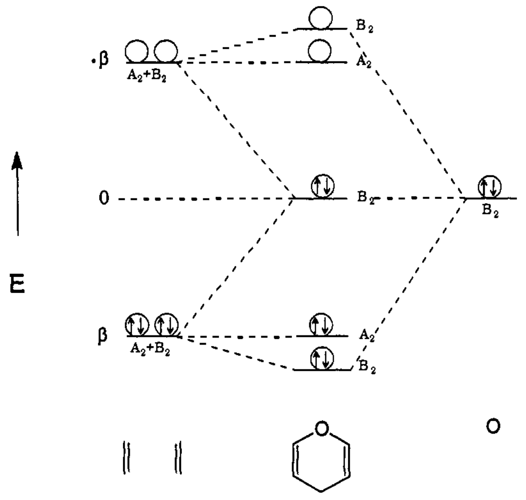

Figure 8. Molecular orbital energy levels for 4*H*-pyran (II) from the modified Hückel calculation.

a stabilization (which is maximum for the planar structure) of $[(\beta^2 + 2\beta_w^2)^{1/2} - \beta]$ results. This is equal to 0.061β when $\beta = \beta_w/4$.

Conclusion

In this work we have determined the ring-puckering potential energy function of 4*H*-pyran from the far-infrared spectrum and the calculation of the kinetic energy expansion. This function clearly indicates that the equilibrium structure of 4*H*-pyran is planar. This is also true for 1,4-cyclohexadiene and 1,4-dioxin. Plausible adjustment of MM3 parameters, verified by modified Hückel calculations, allows good agreement to be obtained between the experimental and calculated potential energy functions. The agreement results when a small π interaction involving nonbonding p orbitals on the oxygen atoms is involved.

The old literature, including organic chemistry textbooks, often described the molecules considered here as having boat conformations so that C–C–C or C–O–C angles could become tetrahedral. It is hoped that the work described here provides a better understanding for why they are in fact planar.

Acknowledgment. J.C. and J.L. thank the National Science Foundation, the Robert Welch Foundation, and the Texas ARP program for financial support. Support from the NIH-Biomedical program (R.M. and J.R.V.) is also gratefully acknowledged.